UPDATES doi.org/10.1002/adsc.202401437 ADVANCED SYNTHESIS & CATALYSIS

Insight into the Key Factors that Influence the Reaction Pathways in the Silyl-Prins Cyclization of *gem*-Vinylsilyl Alcohols

Paula González-Andrés,[a] Carlos Díez-Poza,[a] Laura F. Peña,[a] Daniel Gónzalez-Pinardo,[b] Israel Fernández,[b,*] and Asunción Barbero[a,*]

[a] Department of Organic Chemistry, Faculty of Science, University of Valladolid?, 47011 Valladolid, Spain
Phone: +34-983-423013
Fax: +34-983-423013
E-mail: asuncion.barbero@uva.es

[b] Departamento de Química Orgánica y Centro de Innovación en Química Avanzada (ORFEO-CINQA), Facultad de Ciencias Químicas, Universidad Complutense de Madrid, 28040-Madrid, Spain
Phone: +34-3944312
E-mail: israel@quim.ucm.es

Manuscript received: November 19, 2024; Revised manuscript received: December 10, 2024;
Version of record online: January 2, 2025

Supporting information for this article is available on the WWW under https://doi.org/10.1002/adsc.202401437

Abstract: This work provides an in-depth analysis of the factors governing the different reaction pathways in the acid-catalyzed cyclization of *gem*-vinylsilyl alcohols with aldehydes. The study evaluates the impact of both the ligands attached to silicon and the choice of the Lewis acid on the reaction outcome. Additionally, computational studies offer valuable insights into the mechanism that control these distinct pathways. The process enables the chemo- and stereocontrolled formation of a variety of structural frameworks, offering significant potential for the generation of a broad range of molecular architectures.

Keywords: Prins cyclization; organosilanes; computational studies; Lewis acids; Stereocontrol

Introduction

The fine art of Organic Synthesis has the extraordinary power of replicating some of the most fascinating molecules that nature produces. Some of these substances have changed our everyday lives by providing candidates for pharmaceutical, agriculture, cosmetic, or high-technology applications, among others. But probably medical science is the field that has concentrated more efforts in the search for biologically active molecules. Moreover, Organic Synthesis has proven invaluable for constructing analogues or derivatives of natural products, which can sometimes exhibit enhanced biological properties compared to their natural counterparts.

One of the most abundant scaffolds in biologically active compounds is the tetrahydropyran motif,[1,2] and, therefore, developing methodologies for the preparation of this structural core with a range of substituents over its periphery remains a key objective in Organic Synthesis.[3,4] Additionally, the discovery of methodologies that, depending on the nature of the substrates or catalysts, may follow different reaction pathways, and therefore may afford the construction of structurally diverse scaffolds, is highly desirable. Such methods provide ample possibilities for designing structural variation in target molecules and enhance the potential for novel drug discovery.

Within the various available methodologies for generating oxygen- or nitrogen-containing heterocycles, the Prins cyclization has emerged as one of the most efficient approaches.[5,6] The cyclization involves the acid-catalyzed intramolecular addition of a π-donor group (typically an alkene) to an oxocarbenium ion (generated *in situ* by condensation of the hydroxy group of the starting alkenol with an aldehyde). Several modifications of the Prins cyclization have

been developed by varying the nature of the π-donor or acceptor entities. In recent years, our research has focused on exploring various strategies for synthesizing oxa- and azacycles through silyl-Prins cyclization,[7,8] with particular emphasis on using alkenyl silanes as activated π-donor groups. This method, known as silyl-Prins cyclization, presents multiple benefits, such as enhanced reaction selectivity and a reduction in the formation of unwanted by-products.[9]

Worth of note is the recently published discovery of a tandem silyl-Prins cyclization-aryl migration protocol which occurs with the maintenance of the silyl group in the molecule and aryl migration from silicon to the neighbouring carbon.[10] An even more intriguing finding was that the aryl migration depended on the nature of the acid catalyst (TMSOTf *vs* $BiCl_3$/TMSCl)[11] (Scheme 1).

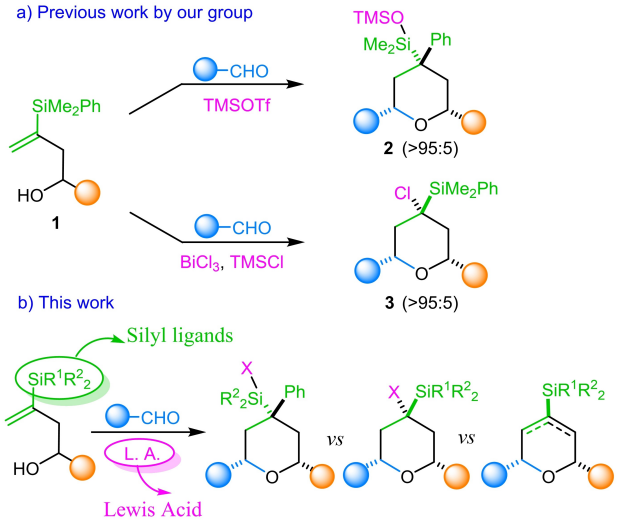

Scheme 1. Previous results and this work.

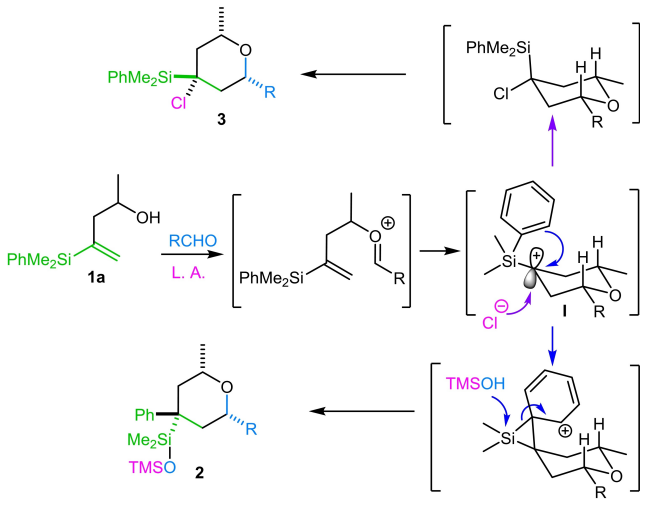

Scheme 2. Proposed mechanism.

The mechanism that we have proposed for these transformations involves the initial formation of an oxocarbenium ion which will then undergo nucleophilic attack by the vinylsilyl group to give an α to silicon carbocation **I** (which is more stable than the corresponding β-silyl carbocation).[12] From this common intermediate, depending on the nature of the Lewis acid counterion, the reaction will evolve with either 1,2-aryl migration from silicon to carbon and final silyl cation trapping by trimethylsilanol (when TMSOTf is used), or by direct nucleophilic trapping of the tertiary carbocation (in the reaction mediated by $BiCl_3$, TMSCl) (Scheme 2).

We envisioned that a better understanding of the factors governing these alternative pathways was required to further develop this synthetically useful transformation. We herein present a deeper overview of this intriguing methodology, highlighting the effects of both the nature of the silyl ligands and the Lewis acid component on the outcome of the cyclization (Scheme 1). Moreover, computational studies have been carried out to gain more insight into the aspects influencing the occurrence of the aryl migration and the high stereocontrol observed.

Results and Discussion

Our initial efforts focused on exploring the influence of the ligands attached to silicon on the process. To this end, we performed further experiments involving substrates with different substituents at the silicon center. Bearing in mind that phenyldimethylsilyl derivatives **1** have been previously demonstrated to undergo selective aryl migration, we thought that it would be interesting to investigate the behaviour of alkenylsilyl alcohols bearing either a diphenylalkylsilyl group or a trialkylsilyl group.

Thus, we first tested the reaction with aldehydes of a model substrate **4** with two phenyl groups bonded to silicon (diphenylmethylsilyl group). As expected, the reaction in the presence of TMSOTf provided the adducts of a tandem Prins cyclization-aryl migration protocol. However, there are two key differences compared to the reaction with the analogous alcohol **1** bearing the phenyldimethylsilyl group: (i) the reaction of the diphenylmethylsilyl derivative **4** proceeded more slowly than the precedent one, suggesting that steric hindrance is influencing this process and (ii) the reactions now resulted in an equimolar mixture of epimers at C4 (**5** and **6**) (Scheme 3).

On the other hand, the Prins cyclization of diphenylmethylsilyl alkenol **4** with *p*-chlorobenzaldehyde, in the presence of a mixture of $BiCl_3$ and TMSCl, provided the expected C4 halogenated tetrahydropyran **7** (no phenyl migration is observed) with

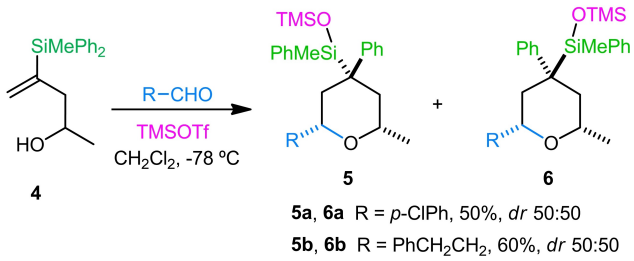

Scheme 3. Effect of the ligands on silicon: diphenylmethylsilyl group and TMSOTf.

stereoselectivity comparable to its phenyldimethylsilyl analog **1**[11] (Scheme 4).

Next, we decided to test the cyclization using the vinylsilyl alcohol **8** with three alkyl groups bonded to silicon. Although the higher migratory aptitude of aryl *vs* alkyl groups is well known, we reasoned that the presence of a primary alkyl group attached to silicon, with higher migratory aptitude than the methyl group, could facilitate the migration. However, no migration was observed in the reaction. Instead, the intermediate

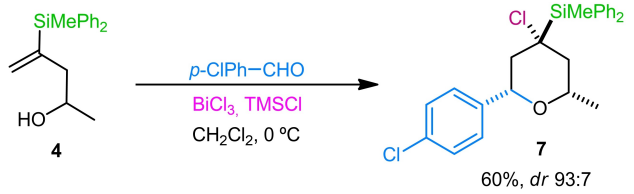

Scheme 4. Effect of the ligands on silicon: diphenylmethylsilyl group and $BiCl_3$/TMSCl.

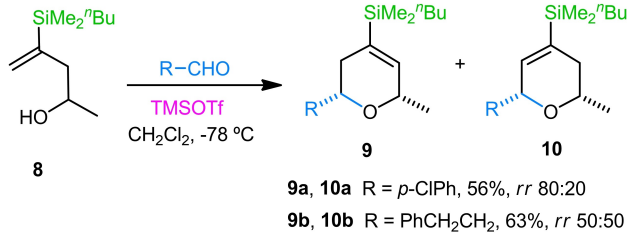

Scheme 5. Effect of the ligands on silicon: trialkylsilyl group and TMSOTf.

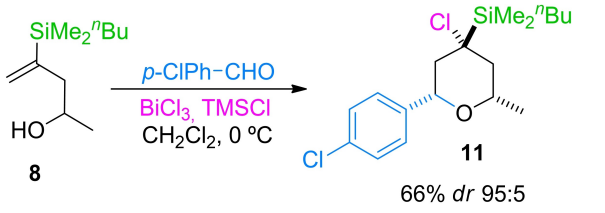

Scheme 6. Effect of the ligands on silicon: trialkylsilyl group and $BiCl_3$/TMSCl.

tertiary cation **I** now undergoes a competitive elimination reaction (**9**, **10**), rather than nucleophilic addition, probably due to the steric requirement of the nucleophile (TMSOH) (Scheme 5).

In line with this hypothesis and with previous results, the cyclization of the trialkylsilyl derivative **8** with *p*-chlorobenzaldehyde, mediated by $BiCl_3$/TMSCl, furnished the expected 4-chorotetrahydropyran **11** in good yield and with excellent stereocontrol (Scheme 6).

These results demonstrate that the cyclization of *gem*-vinylsilyl alcohols, mediated by TMSOTf, undergo a tandem Prins cyclization-aryl migration, provided that the silyl group is attached to an aryl group. However, regardless of the nature of the ligands attached to silicon, when the transformation is mediated by $BiCl_3$/TMSCl, the reaction consistently follows a Prins cyclization pathway.

To gain more insight into the pathways leading to the different outcomes of the transformation, Density Functional Theory (DFT) calculations were carried out at the dispersion corrected PCM(dichloromethane)-B3LYP–D3/def2-TZVPP//PCM(dichloromethane)-B3LYP/def2-SVP level (see computational details in the Supporting Information). To this end, we investigated the process involving the initially formed oxocarbenium ion **INT0** (having the $SiMe_2Ph$ moiety), typically deriving from the reaction of the alcohol fragment to the LA-complexed aldehyde,[13,14] in the presence of either TMSOTf or $BiCl_3$/TMSCl (Figure 1). The initial intermediate **INT0** is, as previously proposed (see above), transformed into the carbocation **INT1** through the intramolecular nucleophilic addition of the vinylsilyl fragment to the electrophilic oxocarbenium. Depending on the conformation of the substituents at the silicon atom, two possible transition states (**TS1**/**TS1'**) and intermediates (**INT1**/**INT1'**) were located on the potential energy surface. Our calculations indicate that the process involving the phenyl group in close proximity to the tetrahydropyran ring (i.e., **TS1**/**INT1**) is favored from both kinetic and thermodynamic points of view. This is mainly due to the occurrence of a stabilizing CH-π non-covalent interaction between the axial hydrogen atoms in the ring and the π-system of the phenyl group as confirmed by the NCIPlot method (see greenish surface in the inset of Figure 1).

In the presence of TMSOTf, intermediates **INT1**/**INT1'** then undergo a 1,2-phenyl migration via **TS2**/**TS2'** (with a low barrier of only ca. 4–5 kcal/mol) to produce the silyl cation intermediates **INT2**/**INT2'**, which after TMSOTf trapping (by the readily formed TMSOH) leads to the observed final products. Once again, the pathway leading to the isomer **INT2'** (via **TS2'**) is kinetically disfavored over the analogous process leading to **INT2**, which is consistent with the experimentally observed preferred formation of the

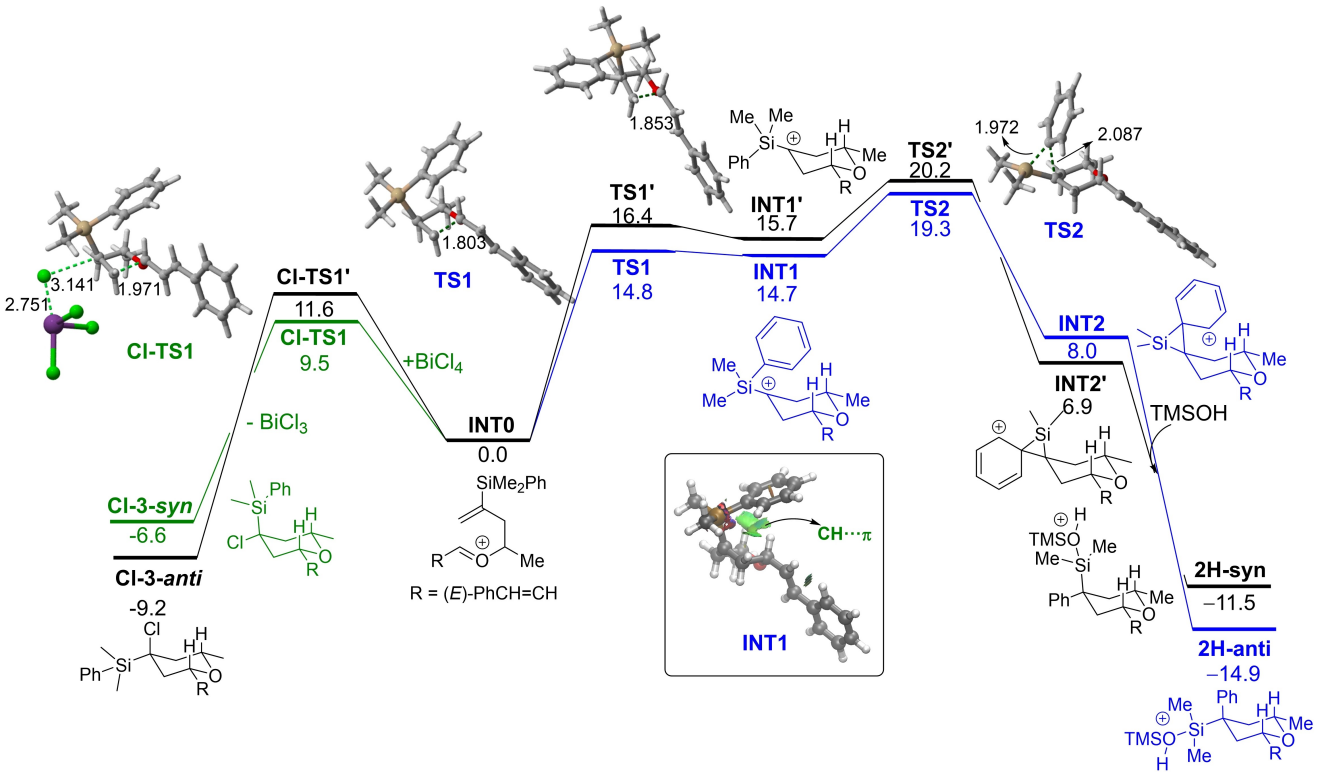

Figure 1. Computed reaction profile for the process involving the initially formed oxocarbenium intermediate **INT0** in the presence of TMSOTf or $BiCl_3$/TMSCl. Relative free energies (ΔG, at 298 K) and bond distances are given in kcal/mol and angstroms, respectively. The inset shows the contour plots of the reduced density gradient isosurfaces (density cutoff of 0.04 a.u.) for **INT1** where the green surfaces indicate attractive non-covalent interactions. All data have been computed at the PCM(dichloromethane)-B3LYP–D3/def2-TZVPP//PCM(dichloromethane)-B3LYP/def2-SVP level.

tetrahydropyran where the phenyl and R groups are placed in *anti*-relative position. On the other hand, in the presence of $BiCl_3$/TMSCl, the formation of $BiCl_4^-$ as the source of chloride can be assumed. Interestingly, we found that the Prins-cyclization and chloride trapping occur in a concerted manner with a lower barrier ($\Delta\Delta G^{\neq}$ ca. 5 kcal/mol) than that computed for the formation of **INT1/INT1'** (i.e., the analogous counteranion-non-assisted process). This is therefore consistent with the exclusive formation of tetrahydropyrans **3** in the processes mediated by $BiCl_3$/TMSCl. In addition, the barrier computed for this concerted cyclization/trapping reaction is lower ($\Delta\Delta G^{\neq}$ = 2.1 kcal/mol) for the process involving **CI-TS1**, where the phenyl group is again placed close to the tetrahydropyran ring. This can be again ascribed to the occurrence of similar CH-π non-covalent interactions in this saddle point. This is also consistent with the preferred formation of the product where the Cl and R substituents are placed in *syn*-relative position (despite being thermodynamically less stable than its anti-counterpart, see Figure 1) and indicates that these weak interactions are key in the selectivity of the process, regardless of the conditions (TMSOTf *vs* $BiCl_3$/TMSCl) used in the experiments.

The divergent outcomes observed in this process prompted us to question whether they can solely be attributed to the nature of the Lewis acid counterion or other factors might also be at play. To explore this further, we decided to study the cyclization using other halides as counterions. Initially, we examined the cyclization reaction of alcohol **1** with cinnamaldehyde, in the presence of bismuth tribromide, which could play the dual role of Lewis acid and source of bromide. However, an unresolved mixture was obtained under these conditions (Table 1, entry 1) and the combination of catalytic $BiBr_3$ with stoichiometric TMSBr did not yield improved results (Table 1, entry 2). Fortunately, reaction mediated by TMSBr in dichloromethane at room temperature afforded the desired 4-bromotetrahydropyran in good yield, although with some inseparable by-products (Table 1, entry 3). By lowering the temperature to −78 °C, we were able to avoid this problem (Table 1, entry 4) and the desired compound was obtained in high yield and as a single product.

In contrast with the slow reaction rates observed with pure TMSCl (which made necessary the addition of $BiCl_3$), the high reactivity of TMSBr obviates the need for additional cocatalysts, such as $BiBr_3$. Moreover, under TMSBr activation, the use of low temper-

Table 1. Optimization for bromide-based Lewis acids.

1a **12**

Entry	Lewis Acid	Solvent	Conditions	Product (yield)
1	$BiBr_3$	CH_2Cl_2	rt, 2 h	UCM[b]
2	$BiBr_3$/TMSBr[a]	CH_2Cl_2	rt, 2 h	UCM[b]
3	TMSBr	CH_2Cl_2	rt, 2 h	**12 j** (74)[c]
4	TMSBr	CH_2Cl_2	−78 °C, 2 h	**12 j** (82)

[a] 0.4 equiv. of $BiBr_3$ and 1.2 equiv. of TMSBr were used.
[b] UCM stands for unresolved complex mixture.
[c] The product could not be separated from other by-products.

ature is required to get selective reactions. Once selected the optimal conditions for this reaction (Table 1, entry 4), we next studied the scope of the process using different aldehydes. The results are shown in Table 2.

The reaction is general for arylic aldehydes (either electron-rich or electron-poor) as well as for vinylic aldehydes. In addition, different substituents (including arylic groups) are tolerated on the carbinol carbon. However, the use of highly reactive aldehydes (i.e., alkylic aldehydes or *p*-nitrobenzaldehyde) resulted in complex mixtures from which it was difficult to isolate the corresponding 4-bromotetrahydropyrans. Interestingly, the reaction again occurs with direct trapping of the intermediate α-silyl tetrahydropyranyl cation **I** by the halide (i.e., products of 1,2-phenyl migration were not observed). Furthermore, excellent diastereoselectivity towards a single diastereomer is obtained in all the examples when the reaction was performed at −78 °C (**12 a**–**12 j**). The relative configuration of the tetrahydropyranyl products was determined by the coupling constants in ^{1}H-NMR and NOESY experiments. Moreover, confirmation of that structure was achieved by means of single-crystal X-ray diffraction of compound **12 b** (Figure 2).

To complete our study, and also motivated by the significance of fluorinated compounds in pharmaceutical and radiological applications, we decided to investigate whether the same reaction pathway observed with chloride and bromide metal Lewis acids is also followed when fluoride is used as the counterion. For that purpose, we choose $BF_3{\cdot}OEt_2$ as the activator. The results are shown in Table 3.

As demonstrated, and in contrast with the behaviour of other metal halide Lewis acids, when fluoride is the counterion the reaction seems to follow a tandem silyl-Prins cyclization/phenyl migration pathway. This might suggest that various factors, including steric hindrance and bond strength, play a critical role in

Table 2. Scope of the silyl-Prins cyclization of *gem*-vinylsilyl alcohols **1** with TMSBr.

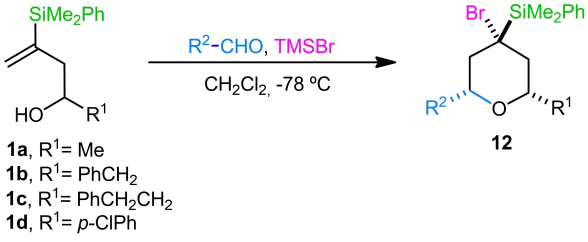

1a, R^1= Me
1b, R^1= $PhCH_2$
1c, R^1= $PhCH_2CH_2$
1d, R^1= *p*-ClPh

12

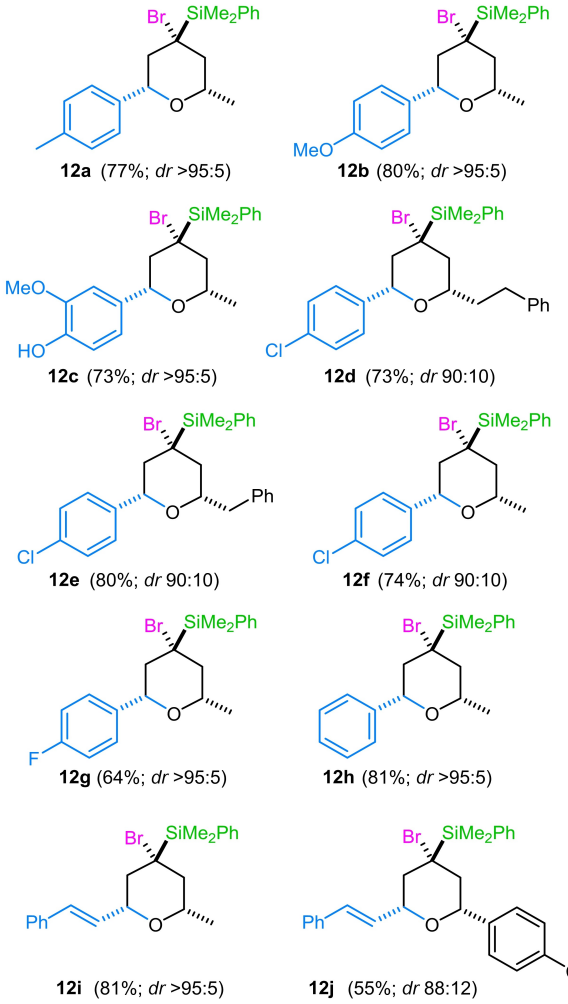

12a (77%; *dr* >95:5)
12b (80%; *dr* >95:5)
12c (73%; *dr* >95:5)
12d (73%; *dr* 90:10)
12e (80%; *dr* 90:10)
12f (74%; *dr* 90:10)
12g (64%; *dr* >95:5)
12h (81%; *dr* >95:5)
12i (81%; *dr* >95:5)
12j (55%; *dr* 88:12)

determining the reaction outcome. The reaction with $BF_3{\cdot}OEt_2$ is effective for both electron-rich and electron-poor aromatic aldehydes, as well as for vinylic aldehydes and even the highly reactive alkylic aldehydes. Additionally, arylic substituents attached to the carbinol are well tolerated, yielding the desired product in moderate yields.

According to our DFT calculations (Figure 3), the concerted Prins-cyclization/fluoride-trapping (with BF_4^- as fluoride source) also proceeds with a lower barrier than the non-assisted process. This leads to the formation of the **F-3-*syn*/*anti*** intermediates with no

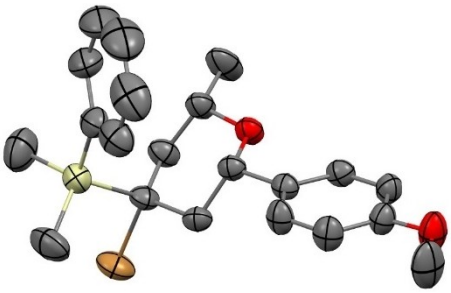

Figure 2. X-ray crystal structure of **12 b**; displacement ellipsoids at 50% probability. H atoms are omitted for clarity. Color key: C (grey), O (red), Si (yellow), Br (orange). CCDC: 2391410.

significant selectivity. From these intermediates, a simultaneous migration of the fluoride and phenyl groups through the C-Si bond takes place to produce the observed tetrahydropyrans. This process therefore can be viewed as a type I dyotropic reaction according to the original definition by M. Reetz.[15,16] Moreover, the dyotropic reaction involving **F-TS2$_{mig}$** is kinetically favored over the analogous process involving **F-TS2$_{mig}$'** ($\Delta\Delta G^{\neq}$ ca. 2 kcal/mol)). This fact, together with the higher thermodynamical stability of the corresponding reaction product, **F-2-*anti***, are responsible for the high stereoselectivity observed experimentally.

Since one of the added values of silicon-containing compounds is their ability to undergo a variety of functional group transformations under mild conditions, we ultimately chose to further investigate the potential of the silylated tetrahydropyrans obtained from this process. To this end, we examined two distinct silicon conversion strategies. We first tested the protodesilylation of adducts from either the cyclization-migration or the cyclization-nucleophilic trapping processes. As shown in Scheme 6, reaction of bromoderivative **12 b** with TBAF in THF gave the corresponding desilylated tetrahydropyran **14** in good yield and with complete retention of the configuration at C4 (Scheme 7).

However, protodesilylation of tetrahydropyrans **2 a** or **13 b**, in which silicon is attached to a very crowded quaternary center,[17,18] yielded desilylated tetrahydropyrans **15** and **16** as a nearly equimolar mixture of diastereoisomers (with either retention or inversion of the configuration at C4) (Scheme 8).

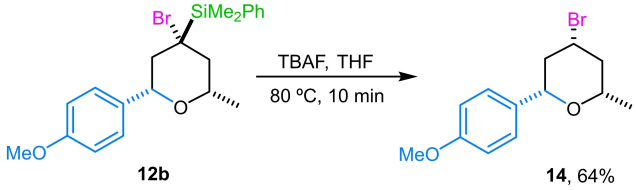

Scheme 7. Protodesilylation process of 4-bromo-4-silyl tetrahydropyran **12 b**.

Table 3. Scope of the silyl-Prins cyclization of *gem*-vinylsilyl alcohols **1** with $BF_3 \cdot OEt_2$.

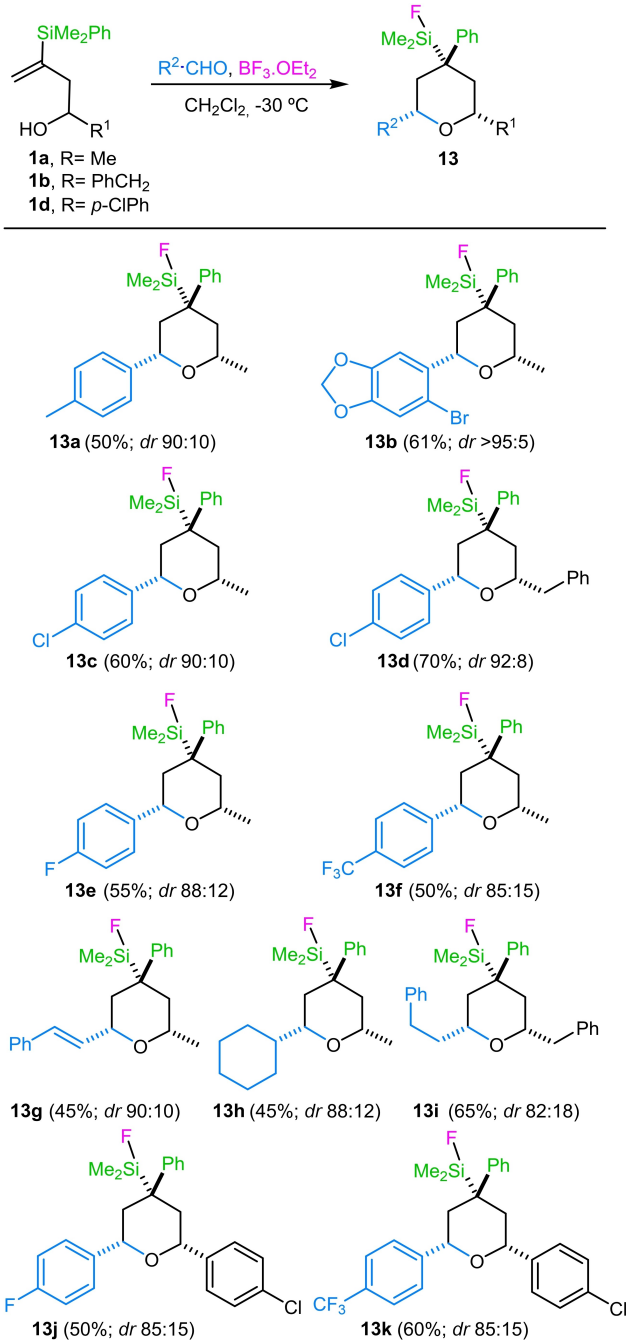

Despite anticipating potential steric hindrance challenges in the Fleming-Tamao oxidation of a silicon-substituted quaternary carbon, we proceeded to evaluate the conversion of the silyl group to a hydroxyl in 4-phenyl-4-silyltetrahydropyrans **2 a** and **13 b**. Attempts to oxidize disilane **2 a** under various conditions,

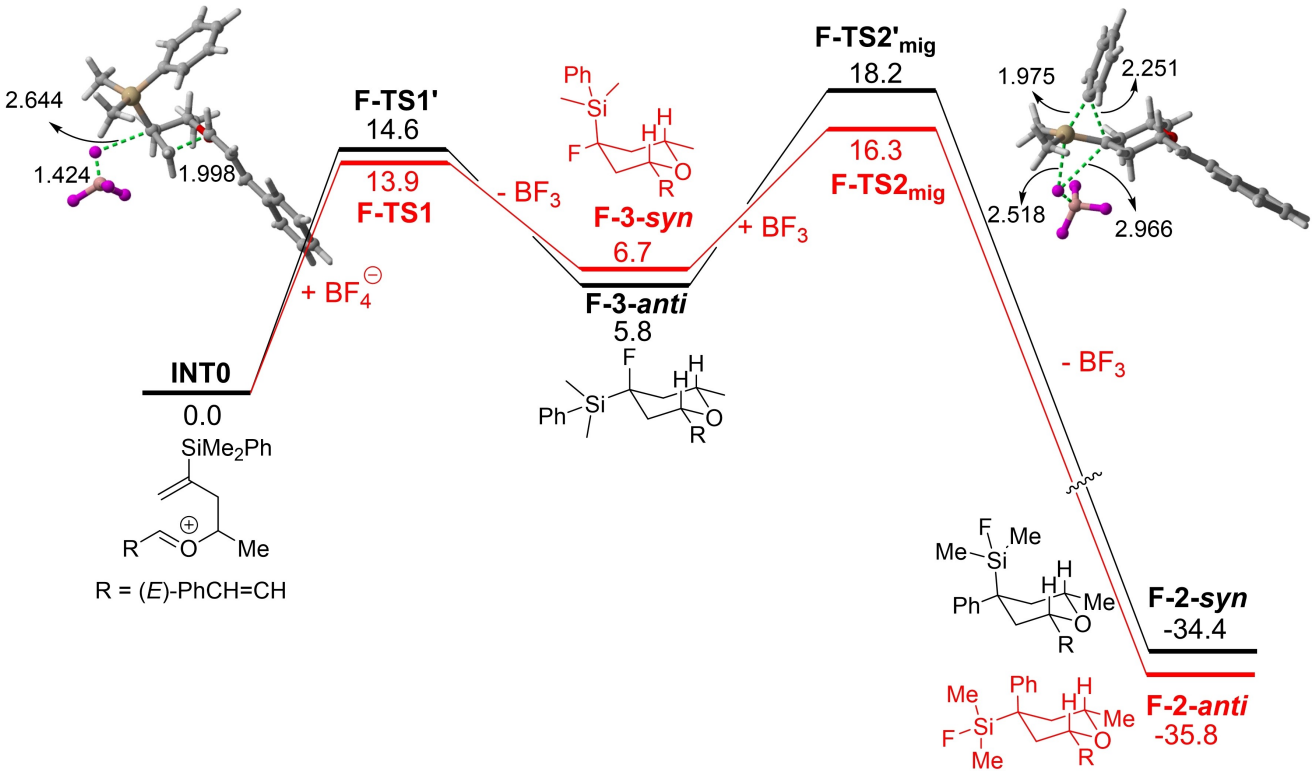

Figure 3. Computed reaction profile for the process involving the initially formed oxocarbenium intermediate **INT0** in the presence of BF_3 as the activator. Relative free energies (ΔG, at 298 K) and bond distances are given in kcal/mol and angstroms, respectively. All data have been computed at the PCM(dichloromethane)-B3LYP–D3/def2-TZVPP//PCM(dichloromethane)-B3LYP/def2-SVP level.

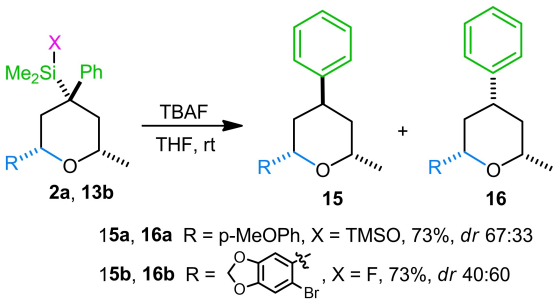

Scheme 8. Protodesilylation of 4-phenyl-4-silyl tetrahydropyrans **2 a** and **13 b**.

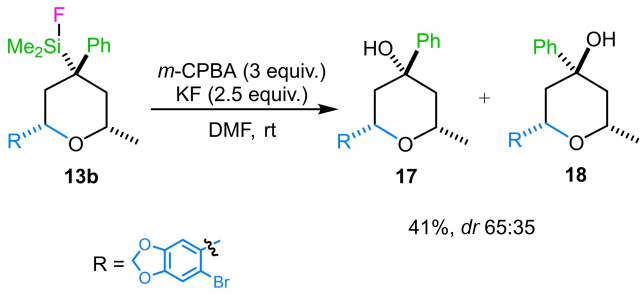

Scheme 9. Fleming-Tamao oxidation of 4-phenyl-4-silyl tetrahydropyran **13 b**.

however, yielded only complex product mixtures. By contrast, the fluorosilane derivative **13 b** demonstrated greater ease of oxidation, producing the desired 4-phenyl-4-hydroxytetrahydropyrans as a mixture of C4 epimers when treated with MCPBA and KF[19] (Scheme 9). Interestingly, tetrahydropyran analogs to compound **17**, bearing aryl groups in C2 and C4, have been reported to exhibit significant tumor growth inhibition in various human cell lines.[20]

Conclusion

A deep examination of the factors controlling the different reaction pathways of the Lewis acid-catalyzed silyl-Prins cyclization of *gem*-vinylsilyl alcohols with aldehydes is provided. The influence on the reaction outcome of both the nature of the Lewis acid and the silicon ligands has been proven. In addition, computational analysis provides a critical insight into the mechanism accounting for the different pathways. Our methodology allows the construction of structurally

diverse scaffolds, presenting considerable promise for the creation of an array of targets.

Experimental Section

Experimental details, characterization data for all new compounds, copies of ^{1}H and $^{13}C\{1\ H\}$ NMR spectra for new compounds and X-ray crystallographic data for compound **12 b** can be found in the Supporting Information.

CCDC-2391410 contains the supplementary crystallographic data for this paper. These data can be obtained free of charge from the Cambridge Crystallographic Data Centre via www.ccdc.cam.ac.uk/structures

Lewis Acid Promoted Cyclization of *gem*-Vinylsilyl Alcohols

A solution of the homoallylic alcohol (1 equiv.) and the corresponding aldehyde (1.2 equiv.) in dry dichloromethane is cooled to the corresponding temperature (under nitrogen). Then, the Lewis acid is dropwise added. The mixture is stirred while monitored by TLC. When starting materials are consumed, it is hydrolyzed with NaOH (aq) 2 M. or sat. $NaHCO_3$. Phases are then separated, extracting the aqueous phase three times with dichloromethane. The organic phases are combined and dried over anhydrous $MgSO_4$. The solvent is then evaporated under reduced pressure. The crude mixture is analyzed by NMR and then purified by column chromatography in silica gel, using mixtures of hexane-ethyl acetate, yielding the corresponding tetrahydropyrans.

Acknowledgements

We are grateful for financial support from grants TED2021-131705B–C21, PID2021-125909OB–I00, PID2022-139318NB–I00 and RED2022-134331-T, funded by MICIU/AEI/10.13039/501100011033 and NextGenerationEU/PRTR. We also acknowledge E. Cuellar for X-ray analysis (Department of Inorganic Chemistry, University of Valladolid, Spain). L. F.-P., P. G.-A. and D. G.-P. acknowledge predoctoral fellowships funded by either the "Junta de Castilla y León", the University of Valladolid or the Comunidad de Madrid.

References

[1] a) D. Kumar, P. Sharma, H. Singh, K. Nepali, G. K. Gupta, S. K. Jain, F. Ntie-Kang, *RSC Adv.* **2017**, *7*, 36977–36999.
[2] N. M. Nasir, K. Ermanis, P. A. Clarke, *Org. Biomol. Chem.* **2014**, *12*, 3323–3335.
[3] A. Shikha, S. Ayushi, S. Jay, S. Nusrat, N. Sahiba, T. Pankaj, *Appl. Organomet. Chem.* **2022**, *36*, e6604.
[4] L. Lempenauer, G. Lemière, E. Duñach, *Adv. Synth. Catal.* **2019**, *361*, 5284–5304.
[5] A. Budakoti, P. K. Mondal, P. Verma, J. Khamrai, *Beilstein J. Org. Chem.* **2021**, *17*, 932–963.
[6] a) C. Olier, M. Kaafarani, S. Gastaldi, M. P. Bertrand, *Tetrahedron* **2010**, *66*, 413–445; b) X. Han, G. Peh, P. E. Floreancig, *Eur. J. Org. Chem.* **2013**, 1193–1208.
[7] a) A. Barbero, A. Diez-Varga, M. Herrero, F. J. Pulido, *J. Org. Chem.* **2016**, *81*, 2704–2712; b) A. Diez-Varga, H. Barbero, F. J. Pulido, A. González-Ortega, A. Barbero, *Chem. Eur. J.* **2014**, *20*, 14112–14119.
[8] a) L. F. Peña, A. Barbero, *Org. Lett.* **2024**, *26*, 5202–5207; b) L. F. Peña, P. González-Andrés, A. Barbero, *RSC Adv.* **2024**, *14*, 707–711.
[9] A. P. Dobbs, S. J. J. Guesne, S. Martinovic, S. J. Coles, M. B. Hursthouse, *J. Org. Chem.* **2003**, *68*, 7880–7883.
[10] C. Díez-Poza, A. Barbero, *Org. Lett.* **2021**, *23*, 8385–8389.
[11] C. Díez-Poza, L. Fernández-Peña, P. González-Andrés, A. Barbero, *J. Org. Chem.* **2023**, *88*, 6776–6783.
[12] T. A. Blumenkopf, L. E. Overman, *Chem. Rev.* **1986**, *86*, 857–873.
[13] S. J. Pérez, M. Purino, P. O. Miranda, V. S. Martín, I. Fernández, J. I. Padrón, *Chem. Eur. J.* **2015**, *21*, 15211–15217.
[14] R. M. Carballo, J. M. Padrón, I. Fernández, D. A. Cruz, L. Grmuša, V. S. Martín, J. I. Padrón, *J. Org. Chem.* **2022**, *87*, 11000–11006.
[15] M. T. Reetz, *Angew. Chem. Int. Ed. Engl.* **1972**, *11*, 129–130.
[16] For a review, see: I. Fernández, F. P. Cossío, M. A. Sierra, *Chem. Rev.* **2009**, *109*, 6687–6711.
[17] G. Maas, M. Alt, D. Mayer, U. Bergsträsser, S. Sklenak, P. Xavier, Y. Apeloig, *Organometallics* **2001**, *20*, 4607–4615.
[18] A. diastereomeric mixture, now enriched in the isomer with inversion of configuration (*dr* 1:3), was obtained when desilylation of **2 a** was done with ^{t}BuOK and 18-crown-6 in DMSO.
[19] K. Tamao, T. Kakui, M. Akita, T. Iwahara, R. Kanatani, J. Yoshida, F. Kumada, *Tetrahedron* **1983**, *39*, 983–990.
[20] P. Singh, A. Bhardwaj, *J. Med. Chem.* **2010**, *53*, 3707–3717.